J. of Supercritical Fluids 98 (2015) 1–11

Contents lists available at ScienceDirect

The Journal of Supercritical Fluids

journal homepage: www.elsevier.com/locate/supflu

Supercritical carbon dioxide fractionation of peppermint oil with low menthol content – Experimental study and simulation analysis for the recovery of piperitenone

Nicolás A. Gañán[a,b,*], J. Sebastián Dambolena[c], Raquel E. Martini[a], Susana B. Bottini[d]

[a] IDTQ – Grupo Vinculado PLAPIQUI – CONICET (Universidad Nacional de Córdoba), Av. Vélez Sarsfield 1611, X5016GCA Córdoba, Argentina
[b] Instituto de Ciencia y Tecnología de los Alimentos – ICTA (FCEFyN – Universidad Nacional de Córdoba), Av. Vélez Sarsfield 1611, X5016GCA Córdoba, Argentina
[c] Instituto Multidisciplinario de Biología Vegetal – IMBiV (Universidad Nacional de Córdoba – CONICET), Av. Vélez Sarsfield 1611, X5016GCA Córdoba, Argentina
[d] Planta Piloto de Ingeniería Química – PLAPIQUI (Universidad Nacional del Sur – CONICET), Camino La Carrindanga Km 7 – CC 717, Bahía Blanca, Argentina

ARTICLE INFO

Article history:
Received 10 October 2014
Received in revised form
18 December 2014
Accepted 19 December 2014
Available online 27 December 2014

Keywords:
Peppermint oil
Supercritical fluid fractionation
GC-EOS
Countercurrent fractionation

ABSTRACT

Low-menthol or dementholized oils can be regarded as potential sources of biocidal compounds, particularly monoterpenic ketones such as menthone, piperitone, piperitenone, pulegone and carvone. In this work, the recovery of piperitenone from peppermint oil by supercritical carbon dioxide fractionation is studied. Separation selectivity and gas loading measurements were performed in a semicontinuous high-pressure apparatus in order to evaluate the effect of temperature and solvent density on these properties. Semicontinuous fractionation was also carried out at a fixed temperature (313 K) and pressure (85 bar), collecting and analyzing extract samples until a purified piperitenone raffinate was obtained. The phase behavior of the system was modeled and predicted with the group contribution equation of state (GC-EOS). Good agreement with the experimental results was obtained. Finally, a continuous countercurrent multistage fractionation process was simulated, based on the GC-EOS model. The effect of operation temperature and pressure, solvent-to-feed ratio and reflux ratio was studied for different purity and recovery requirements and oil feed compositions.

1. Introduction

Peppermint (*Mentha* × *piperita* L.) oil is one of the most important commercial essential oils, along with citrus peel oils, both in production volume and applications. It is used as flavoring agent in the food industry, as well as in fragrance, personal care, cleaning and pharmaceutical industries. During the last decades, peppermint oil world production has oscillated between 2000 and 4000 metric tons per year [1]. It is usually obtained by steam or hydrodistillation of fresh or dried leaves, yielding a volatile product rich in oxygenated monoterpenes, together with small amounts of hydrocarbon monoterpenes and sesquiterpenes. Its commercial value is mainly related to its (−)-menthol content, mint oils being the most common natural source of this compound. Menthol – which is solid at ambient conditions – is generally isolated from the oil by slow crystallization at low temperatures, followed by filtration or centrifugation. The residual liquid is commonly known as "dementholized oil" and its value is considerably lower, although its menthol content can be still as high as 50%.

However, the dementholized oil usually contains several compounds of interest for different applications. For example, menthone can be converted to menthol by catalytic hydrogenation, thus increasing the amount of this compound that can be obtained from the oil. Currently, the main limitation of this process is its low selectivity, yielding a non-specific mixture of stereoisomers of menthol [2,3]. Other components are valuable for their aromatic properties; for example menthyl acetate, menthofuran and 1,8-cineol, which are used in the formulation of fragrances and aromas for giving special or particular notes.

Besides organoleptic applications, mint oils also show biocidal activity against different agricultural and stored product pests and disease vectors, acting as repellents, insecticides, acaricides or antimicrobials [4–7]. Due to this property, combined with increasing environmental and health concerns about synthetic pesticides,

* Corresponding author at: IDTQ – Grupo Vinculado PLAPIQUI – CONICET (Universidad Nacional de Córdoba), Av. Vélez Sarsfield 1611, X5016GCA Córdoba, Argentina. Tel.: +54 351 5353800x29784.
E-mail address: nganan@plapiqui.edu.ar (N.A. Gañán).

http://dx.doi.org/10.1016/j.supflu.2014.12.018
0896-8446/

essential oils and terpenes have gained attention as a potential alternative within the framework of integrated pest management [8,9]. In general, biocidal activity has been attributed to some of the oxygenated constituents, particularly monoterpenic ketones – such as menthone, carvone, pulegone, piperitone and piperitenone [6,10–12]. It has been observed that α,β-unsaturated ketones are generally more active than other ketones, suggesting that this chemical functionality can play an important role in their toxicity [13].

The isolation of the active compounds – or their concentration to a desired level of purity – requires the removal of inactive or less active components of the oil, such as hydrocarbon monoterpenes, which are also unstable and can easily undergo oxidation reactions. This concentration can be performed by conventional methods, such as vacuum distillation (rectification) or liquid extraction. The fractionation with supercritical fluids – particularly carbon dioxide – is an interesting alternative, for several well-known reasons. CO_2 is considered a "green" solvent, because it is not toxic, non-reactive, gaseous at ambient conditions – yielding solvent-free products – and can be easily regenerated and recycled to the process. Moreover, due to its relatively low critical temperature (304 K), operation can be performed at mild conditions, preserving unsaturated compounds from thermal degradation and oxidation.

Fractionation is advantageously carried out in multistage countercurrent columns, which can be operated with different configurations: continuous or semicontinuous, with external or internal reflux, etc. The design and optimization of a fractionation column requires reliable phase equilibrium information, necessary for the selection of suitable conditions that ensure operation within the biphasic region as well as a high selectivity and minimum solvent consumption [14].

Supercritical CO_2 has been applied to the fractionation of essential oils (and synthetic mixtures of terpenes) by many authors, who have reported experimental, modeling and optimization studies. The goal is generally the concentration or purification of a particular compound or fraction, which can be of interest due to organoleptic and/or bioactive properties. The first application case was the deterpenation of citrus peel oils, i.e., the parcial removal of the hydrocarbon monoterpene fraction (mainly limonene) in order to concentrate de valuable oxygenated fraction (linalool, citral), improving the aromatic profile of the oils. Orange and lemon peel oil fractionation has been studied by many authors, providing useful information on the phase equilibrium behavior, separation performance and hydrodynamic aspects of continuous and semicontinuous countercurrent columns [15–19]. These studies have shown that essential oils and terpenic mixtures are readily soluble in supercritical CO_2, and that a good selectivity can be achieved if the operation conditions are properly selected.

Some authors have applied this methodology to the fractionation of herbal essential oils obtained by hydrodistillation, as an alternative to the fractionated supercritical fluid extraction (FSFE) from the plant material. In the case of FSFE, the oil fractions can be successively extracted by changing the extractor conditions (for example, increasing pressure by steps), or can be recovered from the total extract in two or more separation vessels operating in series at different temperature and/or pressure conditions. With this approach, several authors have studied the supercritical fluid extraction of mint essential oils and the subsequent separation of the cuticular waxes from the oil [20–22].

On the other hand, some noteworthy applications of supercritical CO_2 fractionation of herbal essential oils are the purification of aromatic oxygenated monoterpenes (mainly carvacrol) from origanum oil [23], the separation of linalool and linalyl acetate in lavandin oil [24] and the recovery of 1,8-cineol from eucalyptus oil [25]. In previous works, Gañan and Brignole [26,27] have studied the concentration of the oxygenated fraction from essential oils rich in monoterpenic ketones, such as *Salvia officinalis* and *Tagetes minuta* oils, determining recommended operation conditions by experimental studies and computer assisted simulation.

Solubility and phase equilibrium data of main peppermint oil components in supercritical CO_2 has been reported by several authors, namely menthol [28,29], carvone [30], 1,8-cineol [31,32] and hydrocarbon monoterpenes, among others, including also ternary and multicomponent systems. The separation of menthone and menthol as key components in a peppermint oil sample was studied by Gañán and Brignole in a previously cited work [26], concluding that the relative volatility between these compounds was too low in the entire studied range of conditions to allow a practical fractionation.

In this work, the supercritical CO_2 fractionation of a peppermint oil rich in piperitenone is studied. Piperitenone is an α,β-diunsaturated ketone related to menthone. It is also a precursor of piperitenone oxide, a compound which has been reported as an insecticidal, larvicidal, antiviral and antitumoral agent [33]. Based on these facts, the main objective is the purification or concentration of the piperitenone fraction as a model case for the revalorization of dementholized or natural mint oils having low menthol content, regarded as a source of biocidal and biologically active compounds or fractions.

A systematic approach is followed, applying phase equilibrium engineering concepts [34]. Experimental results obtained in a semicontinuous high-pressure apparatus at different temperature and density conditions are presented and discussed in terms of process selectivity and gas loading. The influence of composition is then evaluated by semicontinuous fractionation at fixed temperature and pressure conditions. The phase equilibrium behavior of the CO_2 + peppermint oil system is predicted with the group contribution equation of state (GC-EOS) [35] and compared with experimental results. Based on this thermodynamic model, a continuous countercurrent fractionation column is simulated and analyzed in order to select operating conditions for different process or product quality requirements, providing useful information for the design and optimization of a fractionation process.

2. Materials and methods

2.1. Materials

In this work, a sample of peppermint (*Mentha* × *piperita* L.) essential oil rich in piperitenone was used. It was obtained at Universidad Nacional de Córdoba by steam distillation from fresh leaves harvested in the province of Córdoba (Argentina) and was stored at 263 K protected from light. The essential oil composition was determined by gas chromatography and mass spectrometry (GC–MS) following the method described in Section 2.3.

Industrial extra-dry carbon dioxide (≥99.8%, Linde, Argentina) was used in the supercritical fluid fractionation experiments. Methanol (≥99.8%, HPLC grade, Sintorgan, Argentina) was used for the recovery of the extracted fractions and samples. Ethanol (95%, v/v, food grade, Porta, Argentina) was used for cleaning the experimental apparatus and for the recovery of residues.

2.2. Experimental setup and procedure

Equilibrium and fractionation experiments were performed in a lab-scale semicontinuous apparatus schematically described in Fig. 1. It consists of a high-pressure column of 30 cm^3 of internal volume (1.1 cm inner diameter, 32 cm height), filled with 1 mm-diameter glass spheres, where the oil sample (1 cm^3) is loaded. The column is kept at constant temperature by an external aluminium jacket heated by electrical resistances and connected to

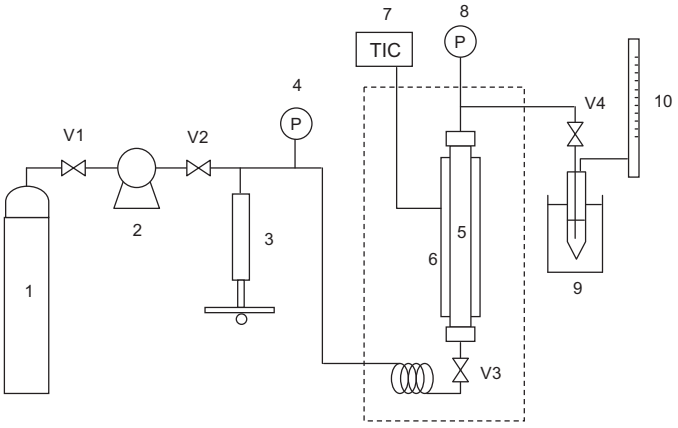

Fig. 1. Experimental apparatus. 1, CO_2 tank; 2, high-pressure liquid pump; 3, pressure generator; 4, manometer; 5, high-pressure extraction column; 6, aluminium heating jacket; 7, temperature controller; 8, pressure transducer; 9, solute trap; 10, bubble gas meter; V, valves.

a temperature controller (DH-101, Dhacel, Argentina). After loading the oil, CO_2 is fed to the system through a high-pressure liquid pump (Waters 501, Millipore, USA) up to the desired pressure value, measured by a pressure transducer (CS-PT300 Xian Chinastar M&C Ltd., China). Pressure was controlled within a range of ±0.5 bar and temperature within a range of ±0.1 K.

After reaching constant temperature and pressure, the system is allowed to equilibrate for at least 3 h, with inlet and outlet valves closed, to ensure equilibrium conditions and saturation of the gas (or supercritical) phase. During equilibration the oil components distribute between the liquid and gas phases according to their volatility and affinity with CO_2. Then, the outlet or expansion valve (V4) is gently opened in order to adjust the gas flow rate to a sufficiently low value (0.1 g/min) to keep equilibrium conditions (dynamic or "gas saturated" method). The exiting gas phase is continuously replaced by fresh CO_2 using a pressure generator, with valve V3 opened. After depressurization, the solutes dissolved in the gas stream are condensed and collected in a solute trap. The CO_2 flow rate is measured and controlled using a bubble gas meter connected to the outlet of the solute trap. The accuracy of the gas meter column is 0.1 cm^3. This procedure has been already tested in a similar device described in the above mentioned previous works [26,27] and validated by reproduction of solubility and fractionation data reported in the literature for the system CO_2 + lemon peel oil.

The solute samples were collected using two alternative methods: (a) by bubbling the gas stream in a closed vessel filled with 5 ml of methanol and (b) by direct condensation in a glass U-tube provided with glass wool in the exit shoulder in order to minimize extract losses. In both cases, the solute traps were kept refrigerated at 250 K by means of a thermostatic bath (RE-107, Lauda, Germany). The mass of the glass U-tubes is in the range of 17–19 g, and the typical mass of the collected extract samples is in the range of 20–50 mg. In the first method the solution is directly analyzed by GC, while in case (b) the condensed solutes are dissolved in methanol prior to analysis. Direct condensation allowed determining the gas loading (or oil solubility) gravimetrically, by weighing the U-tube before and after the extract recovery in an analytical balance (Ohaus Adventurer Pro, New Jersey, USA, d = 0.1 mg). The amount of CO_2 is calculated volumetrically by integrating the flow rate measurements over time and by subsequent conversion of the calculated volume to mass, at room temperature, pressure and humidity conditions. The gas flow rate was checked every 1–2 min along each run, in order to minimize integration errors. Once the flow rate was stabilized, the variation was very low (<5%). The samples obtained by bubbling were used for determining the composition of the extract phase, which was in good agreement with the composition of the samples obtained by condensation, showing that both methods were consistent.

Two kinds of experiment were conducted. In the *equilibrium* measurements only a small sample of the gas phase was extracted at fixed temperature and pressure conditions. The aim of these experiments was to determine the composition of the gas phase in equilibrium with the liquid feed (essential oil) at different conditions, as well as the gas loading or "global solubility".

In the *fractionation* experiments the sample of oil was continuously (and selectively) extracted until total or partial removal of the more volatile components, at fixed temperature and pressure conditions. Samples were successively collected and analyzed, in order to track the gas phase composition during the whole fractionation process. These experiments can also provide information about how the relative volatility depends on the system global composition (at fixed temperature and pressure conditions), as it is continuously changing during the extraction. After reaching the desired degree of extraction, pressure was raised up to 150 bar, in order to dissolve and extract the residual liquid or raffinate (piperitenone-rich fraction).

2.3. Chromatographic analysis

The characterization of the peppermint essential oil was performed in a gas chromatograph (Clarus 600, Perkin Elmer, USA) coupled with an ion trap mass detector (GC–MS) and equipped with a capillary column DB-5 (60 m × 0.25 mm i.d. and 0.25 μm film thickness). The temperature of the column was programmed to increase from 333 to 513 K at a rate of 4 K/min. Detector and injector temperatures were set at 523 K. Helium was used as carrier gas at a flow rate of 0.9 ml/min. Ionization was achieved by electron impact at 70 eV. Mass spectral data were acquired in the scan mode in the m/z range 35–250. Retention indices (RI) of the oil components were determined on the basis of homologous n-alkane hydrocarbons under the same conditions. The compounds were identified by comparing their retention indices and mass spectra with published data [36] and available libraries (NIST).

The quantitative analysis of the oil and the extract samples obtained in the different experiments was performed in a gas chromatograph (Clarus 500, Perkin Elmer, USA) equipped with a flame ionization detector (GC–FID), using the same column and temperature program as for GC–MS. In all cases, samples were diluted with methanol and the injection volume was 1 μl. The quantitative composition was obtained by peak area normalization, and the response factor for each component was considered equal to 1.

3. Modeling

3.1. Thermodynamic model: GC-EOS

The thermodynamic behavior of the CO_2 + peppermint oil system was modeled with the group contribution equation of state (GC-EOS) [35]. This equation is particularly suitable for the description and prediction of the phase behavior of natural complex mixtures using a limited number of group parameters, and has been successfully applied to the description of CO_2 + terpenic systems by several authors [19,26,27,37,38].

The essential oil is represented here as a pseudo-binary mixture of 1,8-cineol and piperitenone. The selection of these key components is based on their abundance and volatility behavior, as explained in Section 4. The chemical structure of these compounds is shown in Fig. 2 and their group structure is presented in Table 1. The relevant physico-chemical properties (molar mass,

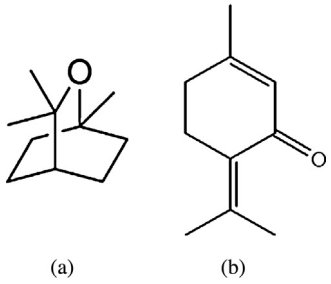

Fig. 2. Chemical structure of oil key components. (a) 1,8-Cineol, (b) piperitenone.

Table 1
Group structure of key components.

Group	CO_2	1,8-cineol	Piperitenone
CH_3	–	–	3
CH_3(B)	–	3	–
$CYCH_2$	–	4	2
CYCH	–	1	–
C=CH	–	–	2
CH_2—O	–	1	–
CH_2C=O	–	–	1
CO_2	1	–	–

Table 2
Physicochemical properties of key components.

	M_W (g/mole)	T_c (K)	P_c (bar)	NBP (K)
CO_2	44.0	304.2	72.8	–
1,8-Cineol	154.3	796.1	27.3	450.2
Piperitenone	150.2	777.3	28.9	512.2

critical temperature and pressure, normal boiling point) are shown in Table 2. Critical properties were estimated using Joback's group contribution method [39]. The pure group, binary interaction and binary non-randomness parameters used in the model are reported in Tables 3–5. All the available parameters were used, according to the most recent update [40]. The number of surface segments q of the ketone and ether groups was modified in order to account for the lack of one or more H atoms, thus avoiding the definition of new groups. The binary interaction and non-randomness parameters of these groups were not modified. The correlated binary parameters

Table 3
GC-EOS pure group parameters.

Group	T^*	q	g	g'	g''
CH_3	600.0	0.848	316910	−0.9274	0
CH_3(B)	600.0	0.789	316910	−0.9274	0
$CYCH_2$	600.0	0.540	466550	−0.6062	0
CYCH	600.0	0.228	466550	−0.6062	0
C=CH	600.0	0.676[a]	546780	−1.0966	0
CH_2—O—	600.0	0.240[b]	503700	−0.9821	0
CH_2C=O	600.0	0.640[b]	888410	−0.7018	0
CO_2	304.2	1.261	531890	−0.5780	0

[a] q = 0.485 for the C=C group of piperitenone.
[b] Modified in order to account for the lack of one or more H atoms.

for the interaction between the ketone and olefinic groups were reported in a previous work [26]. The binary parameters between the ether group and cyclic paraffin, olefin and ketone groups are not available. In a first approach, they were given ideal values. As a globally good agreement between predictions and experimental results was achieved upon this consideration, these ideal values were kept. The calculations were then completely predictive, as no information from our experiments was used in the estimation of the model parameters.

Solubility prediction of the key components in near critical and supercritical carbon dioxide was verified against binary data reported in the literature [30–32]. As can be seen in Fig. 3, solubility prediction for 1,8-cineol is in fair agreement with experimental data at 318 K, with higher deviation at 323 and 333 K. However, it has to be noticed that the data points at these temperatures are somewhat scattered. To the best of our knowledge, there is no information in the literature concerning solubility or phase equilibrium data of piperitenone. Therefore, the comparison was made with data for the isomeric ketone carvone, also a diunsaturated monoterpenic ketone with a similar group structure and close boiling point (504.2 K). In this case, GC-EOS predictions are in good agreement with literature data at 312 and 322 K, as shown in Fig. 4.

3.2. Semicontinuous fractionation

From the standpoint of the oil components (i.e., on a solvent-free basis), the semicontinuous fractionation process can be analyzed as a batch distillation. This process is mathematically described by the well-known Rayleigh equation, which is essentially a component

Table 4
Binary interaction parameters (k_{ij} above diagonal, k'_{ij} below diagonal).

Group	CH_3	CH_3(B)	$CYCH_2$	CYCH	C=CH	CH_2—O	CH_2C=O	CO_2
CH_3	1	1	1	1	1	0.924	0.834	0.892
CH_3(B)	0	1	1	1	1	0.924	0.834	0.892
$CYCH_2$	0	0	1	1	1	1	0.870	0.928
CYCH	0	0	0	1	1	1	0.870	0.928
C=CH	0	0	0	0	1	1	0.975	1
CH_2—O—	−0.056	−0.056	0	0	0	1	1	1.042
CH_2C=O	0.084	0.084	0.097	0.097	0	0	1	1.025
CO_2	0	0	0.210	0.210	0	0	0.108	1

Table 5
Binary non-randomness parameters (α_{ij} above diagonal, α_{ji} below diagonal).

Group	CH_3	CH_3(B)	$CYCH_2$	CYCH	C=CH	CH_2—O	CH_2C=O	CO_2
CH_3	0	0	0	0	0	0	0.854	3.369
CH_3(B)	0	0	0	0	0	0	0.854	3.369
$CYCH_2$	0	0	0	0	0	0	0.854	0
CYCH	0	0	0	0	0	0	0.854	0
C=CH	0	0	0	0	0	0	0	0
CH_2—O—	0	0	0	0	0	0	0	0
CH_2C=O	5.146	5.146	5.146	5.146	0	0	0	0.170
CO_2	3.369	3.369	0	0	0	0	0.170	0

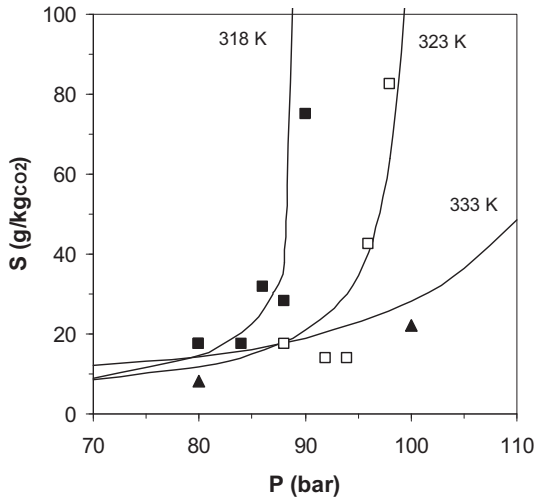

Fig. 3. Solubility of 1,8-cineol in supercritical CO_2 as a function of temperature and pressure. Experimental data: (■) T = 318 K, (□) T = 323 K [32], (▲) T = 333 K [31], (—) GC-EOS predictions.

mass balance. For a binary system, this equation can be easily solved to the following expression:

$$\ln\left(\frac{W_0}{W}\right) = \frac{1}{\alpha - 1}\left[\ln\left(\frac{x_0}{x}\right) + \alpha \ln\left(\frac{1-x}{1-x_0}\right)\right] \quad (1)$$

where W_0 and W are the moles of liquid feed (oil) at the beginning of the process and at a given time t, respectively, and x_0 and x are the corresponding compositions of the volatile component in this liquid-phase [41]. This equation contains only one parameter: the relative volatility between the volatile and the heavy component (α), which is assumed composition-independent and therefore constant during the whole process. It can be obtained experimentally or predicted by a reliable equation of state or other suitable method.

In this work, the Rayleigh equation was applied to the simulation of the pseudo-binary semicontinuous fractionation of peppermint oil, using the experimental value of the relative volatility. On the other hand, calculations with a composition-dependent relative volatility predicted with the GC-EOS model were also performed. In this case, the fractionation process was simulated by a series of successive flash calculations at fixed temperature and pressure

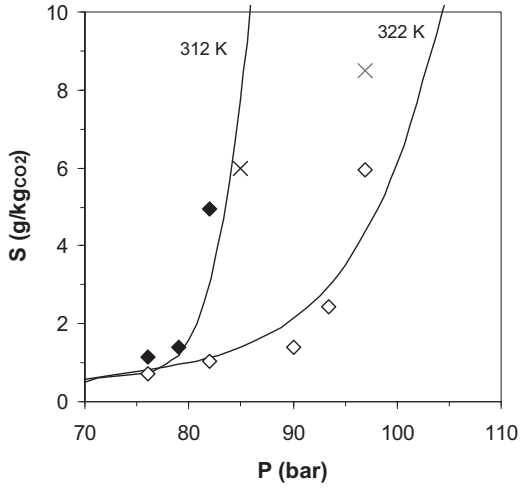

Fig. 4. Solubility of carvone in supercritical CO_2 as a function of temperature and pressure. Experimental data: (♦) T = 312 K, (◊) T = 322 K [30], (×) solubility of peppermint oil (this work), (—) GC-EOS predictions.

Table 6
Peppermint essential oil composition.

Component	RI	M (g/mole)	% GC area
α-Pinene	933	136.2	1.69
Sabinene	972	136.2	1.33
β-Pinene	978	136.2	2.61
β-Myrcene	986	136.2	3.96
1,8-Cineol	1035	154.3	20.28
(−)-Menthone	1159	154.3	0.95
(−)-Menthol	1182	156.3	1.58
Isopiperitenone	1274	152.2	1.04
Piperitenone	1353	152.2	61.15
β-Caryophyllene	1427	204.4	2.22
D-Germacrene	1488	236.4	3.18

conditions [42], taking into account the global composition changes at each extraction step.

3.3. Continuous countercurrent fractionation

A multistage countercurrent fractionation column was simulated using the subroutine GCEXTRAC, a robust simulator of a high-pressure extractor supported by the GC-EOS thermodynamic model [43]. It has been applied to the simulation and optimization of several supercritical fluid fractionation processes, such as the deterpenation of citrus peel oils [19], the extraction of solvents and pollutants from edible oils [44] and the fractionation of fish oil ethyl esters [45], among others.

In this case, a 10-stage isothermal column was simulated, with solvent feed at the bottom and oil feed at the top (simple countercurrent) or at an intermediate stage, with partial recycle of the extract product at the top stage (external reflux).

Besides temperature and pressure conditions, the effect of other variables such as the solvent-to-feed ratio (S/F) and the reflux ratio (RR) was investigated, and appropriate operation conditions were chosen in order to meet specified piperitenone purity and recovery requirements. Solvent consumption and investment costs were additional criteria taken into consideration.

4. Results and discussion

4.1. Selectivity and gas loading measurements

Peppermint oil composition (determined by gas chromatography) is presented in Table 6. Piperitenone and 1,8-cineol are the main components, making up about 80% wt. of the oil. Hydrocarbon monoterpenes and sesquiterpenes account for approx. 10% wt. and 5% wt. of the oil, respectively.

In order to investigate the influence of temperature and CO_2 density on the separation selectivity and gas loading, equilibrium measurements were performed according to the dynamic method described in Section 2.1. Three experimental conditions were selected: (i) 313 K and 85 bar, (ii) 323 K and 97 bar, (iii) 323 K and 120 bar. Conditions (i) and (ii) correspond to a similar pure CO_2 density of ~350 kg/m^3, while condition (iii) corresponds to a CO_2 density of ~580 kg/m^3, according to data reported by NIST [46]. In this way, the effects of temperature and density were evaluated separately with a minimum number of experimental runs, due to limited availability of essential oil. The experiment (i) was performed by duplicate, in order to assess the experimental error.

For each experimental condition, the extract-phase composition in terms of CO_2-free mass fraction is shown in Table 7. Distribution coefficients for each component on a solvent-free basis (K_i') are also presented as a measure of their volatility. Each K_i' is calculated as the ratio between the concentration of component i in

Table 7
Extract-phase composition (% wt., CO_2-free), distribution coefficients (K_i'), relative volatility (α_{12}) and gas loading at different operation conditions.

Component	313 K/85 bar (ρ = 350 kg/m^3)		323 K/97 bar (ρ = 350 kg/m^3)		323 K/120 bar (ρ = 580 kg/m^3)	
	% area	K_i'	% area	K_i'	% area	K_i'
α-Pinene	5.47	3.24	4.92	2.91	2.00	1.18
Sabinene	2.53	1.90	3.65	2.74	1.95	1.47
β-Pinene	6.87	2.63	4.39	1.68	2.63	1.01
β-Myrcene	10.58	2.67	8.26	2.09	4.48	1.13
1,8-Cineol	41.43	2.04	35.53	1.75	26.37	1.30
(−)-Menthone	1.30	1.37	1.23	1.29	1.45	1.53
(−)-Menthol	0.88	0.56	1.89	1.20	1.86	1.18
Isopiperitenone	0.40	0.38	0.84	0.81	0.93	0.89
Piperitenone	27.24	0.45	35.86	0.59	50.05	0.82
β-Caryophyllene	1.66	0.75	2.22	1.00	3.54	1.59
D-Germacrene	1.64	0.52	1.93	0.61	4.74	1.49
Total fraction 1	68.18	2.21	59.87	1.94	40.74	1.32
Total fraction 2	31.82	0.46	40.13	0.58	59.26	0.86
Relative volatility (α_{12})	–	4.81	–	3.35	–	1.54
Gas loading (g/kg CO_2)	–	6.0	–	8.5	–	33.5

the extract-phase and its concentration in the natural oil, which is considered approximately equal to the CO_2-free composition of the liquid phase. Two different groups of components can be recognized in terms of their relative volatility: a more volatile fraction 1, rich in 1,8-cineol, which tends to concentrate in the gas phase ($K_i' > 1$) and a less volatile fraction 2, rich in piperitenone, which tends to remain in the liquid phase ($K_i' < 1$). Based on this consideration, the relative volatility of fraction 1 with respect to fraction 2 (α_{12}) is calculated as a measure of the fractionation selectivity. Gas loading (or global oil solubility) results are also reported. The experimental error estimation was ±0.5 for the relative volatility and ±1.4 g/kg for the gas loading, based on the duplication of the experiment at 85 bar and 313 K.

Although 1,8-cineol and piperitenone are polar molecules (due to the presence of oxygenated functions) and have approximately the same molar mass, they show a significant difference in vapor pressure, as reflected by their boiling points (Table 2), being 1,8-cineol closer to hydrocarbon monoterpenes. This could be explained in terms of their molecular configuration: as the bicyclic structure gives 1,8-cineol a more "spherical" shape, piperitenone is a rather "planar" molecule due to the conjugated double bonds, as can be seen in Fig. 2. This particular behavior of 1,8-cineol has been observed by other authors. Matos and Gomes de Acevedo [32] have reported that the solubility of 1,8-cineol in dense CO_2 is similar to the solubility of limonene (a typical hydrocarbon monoterpene) and that no selectivity between them can be obtained. Francisco and Sívik [31] have pointed the same conclusion regarding the separation of an equimolar mixture of limonene and 1,8-cineol with supercritical CO_2 in the context of eucalyptus oil fractionation. In a previously cited work, Gañán and Brignole [26] have also observed that 1,8-cineol volatility behavior in supercritical CO_2 was closer to the monoterpene fraction than to the ketone fraction during the fractionation of *S. officinalis* essential oil.

From Table 7, it can be seen that increasing temperature at constant CO_2 density (~350 kg/m^3) enhances gas loading (from 6 g/kg at 313 K to 8.5 g/kg at 323 K) but decreases selectivity, which drops from 4.8 to 3.4. This can be due to a higher influence of temperature on the vapor pressure of piperitenone than for 1,8-cineol (and hydrocarbon monoterpenes). Increasing CO_2 density to ~580 kg/m^3 at constant temperature (323 K) has the same effect, with a remarkable increase in gas loading but an almost complete loss of selectivity. This opposite behavior of selectivity and gas loading is a well-known phenomenon in supercritical fluid fractionation, and usually leads to a trade-off between product quality, solvent consumption and investment costs.

GC-EOS model predictions are shown in Figs. 5 and 6 together with the experimental results. As mentioned before, the oil was modeled as a pseudo-binary system composed of a more volatile and a less volatile fraction, represented by 1,8-cineol and piperitenone respectively. Fig. 5 shows the changes of relative volatility and gas loading with pressure for the temperature range 313–333 K. Fig. 6 presents the same information, but as a function of pure CO_2 density. It can be seen that the model predicts a nearly exponential increase of gas loading with density and a correlative exponential decrease of selectivity, along with a negligible effect of temperature, only appreciable at low density conditions (below 300 kg/m^3). When represented as a function of pressure instead of CO_2 density, a crossover region is predicted between 80 and 90 bar for the relative volatility as well as for the gas loading isotherms. Quantitatively, the prediction of the experimental results is acceptable in the lower pressure range, but at higher pressure conditions higher relative deviations are obtained (up to 41% for relative volatility and up to 52% for gas loading).

The experimental results, as well as the model predictions, are in agreement with data reported for similar systems. Gas loading values typically observed for terpenic systems (binary or multicomponent) are in the range 1–50 g/kg, with a more pronounced increase with pressure at lower temperatures, until reaching single phase conditions. The pressure limit of the biphasic region increases with temperature. This behavior can be seen in the binary systems CO_2 + 1,8-cineol and CO_2 + carvone shown in Figs. 3 and 4, as well as in the above mentioned works [17,24,26]. The oil composition has also great influence, oils rich in hydrocarbon monoterpenes – like citrus peel oils – being more soluble in supercritical CO_2 than the oils richer in oxygenated compounds, at given temperature and pressure conditions. Regarding relative volatility, typical values for terpenic mixtures are in the range 1–15, depending on the involved compounds and their relative abundance. For example, high selectivity values (~15) were reported for the separation of β-ocimene and ocimenone fractions in *T. minuta* oil at 323 K and 75–80 bar [26], but the selectivity reported between linalool and linalyl acetate fractions in lavandin oil at the same conditions was only about 1.4 [24].

4.2. Semicontinuous fractionation

Based on the previous results, semicontinuous fractionation of peppermint oil was performed at 313 K and 85 bar. Although higher selectivity is expected at lower pressures, density control can be very difficult when operating too close to the CO_2

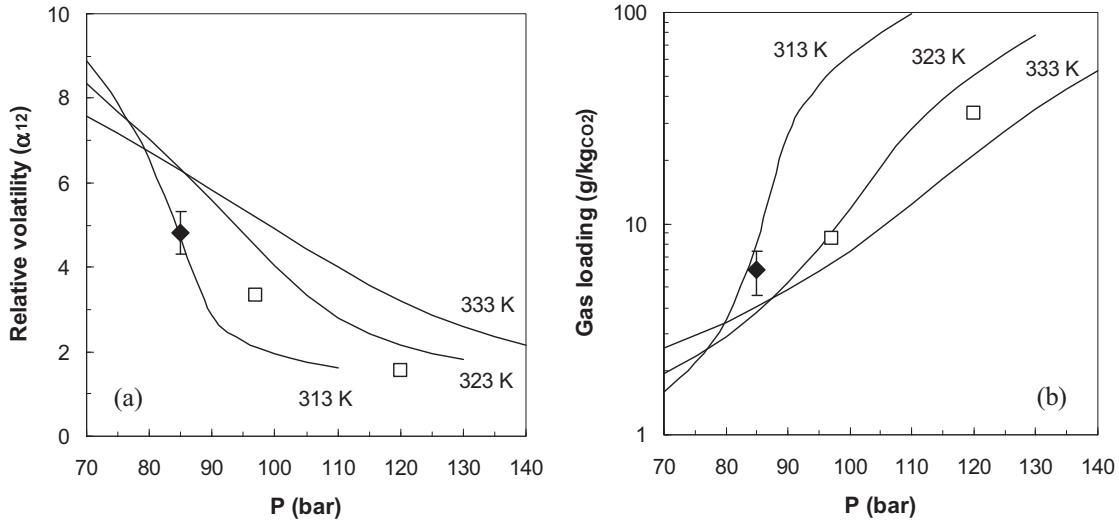

Fig. 5. Relative volatility (a) and gas loading (b) as a function of temperature and pressure. Experimental data: (♦) $T = 313$ K, (□) $T = 323$ K, (—) GC-EOS predictions.

critical region, due to its high sensitivity to small pressure and/or temperature variations. A sample of oil (1 cm^3) was loaded into the high-pressure cell and a continuous stream of CO_2 was fed to remove the more volatile components, leaving a residue (raffinate) enriched in piperitenone. As previously explained, successive samples from the gas (or extract) phase were taken at different intervals and analyzed by gas chromatography.

The gas-phase composition along the fractionation process is shown in Fig. 7(a) as a function of the extraction degree. It can be seen that the composition of the volatile fraction (Y_1, on CO_2-free basis) is initially higher than that in the feed oil (around 0.7), and it continuously decreases as the more volatile compounds are removed and the liquid is enriched in piperitenone. Fractionation was performed until ~55% of the oil sample was extracted. Then, pressure was raised up to 150 bar and the residual liquid or raffinate was recovered, with a residual content of 1,8-cineol of approx. 5% wt.

Fig. 7(a) also shows the predicted behavior calculated with Rayleigh equation. The relative volatility was given a constant value of 4.8, corresponding to the experimental value obtained at these process conditions. It can be seen that the agreement with the experimental data is fairly good, suggesting that the relative volatility does not change significantly with composition along the process. For comparison purposes, the predicted behavior considering a variable relative volatility, recalculated in each step by the GC-EOS model, is also shown.

On the right side, Fig. 7(b) shows the X–Y equilibrium diagram for the volatile molar fractions at process conditions (on a CO_2-free basis). The experimental results were calculated estimating the liquid composition by successive mass balances. The equilibrium curve was calculated using the Rayleigh equation within the entire composition range.

Both diagrams can be used together to analyze the fractionation process of an oil sample for preparative purposes. For example, if a final product with 90% of piperitenone (fraction 2) is required, diagram (b) indicates that this liquid-phase composition is in equilibrium with a gas-phase composition of approx. 40% of 1,8-cineol (fraction 1). According to diagram (a) this gas-phase composition corresponds to approx. 45% of extraction. In this way, the process can be monitored gravimetrically, just by weighing the extracted mass collected in the trap, instead of analyzing several extract samples by gas chromatography. Only one sample has to be analyzed in order to obtain the experimental value of the relative volatility between fractions 1 and 2 at the operation conditions, required for

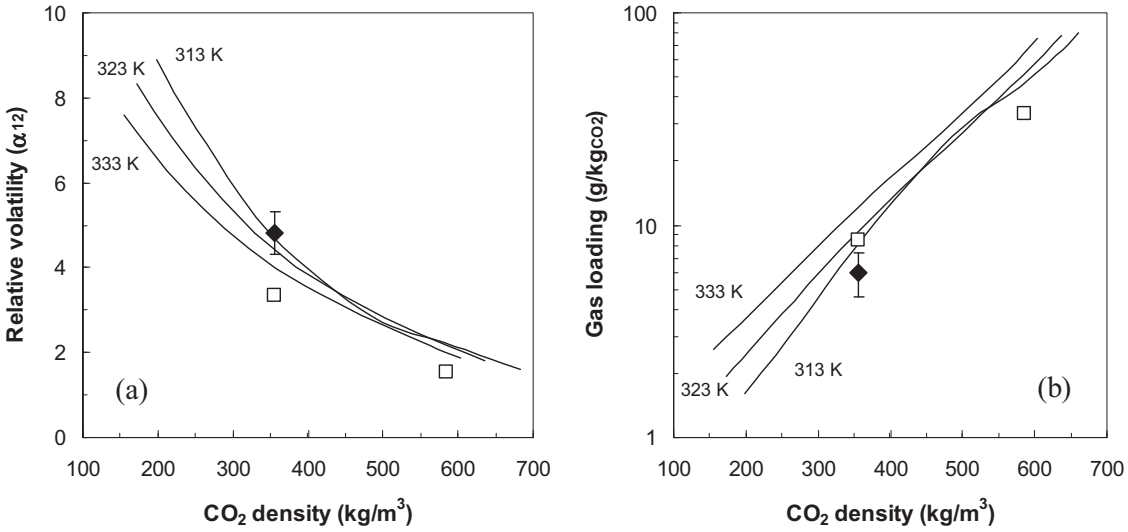

Fig. 6. Relative volatility (a) and gas loading (b) as a function of temperature and pure CO_2 density. Experimental data: (♦) $T = 313$ K, (□) $T = 323$ K, (—) GC-EOS predictions.

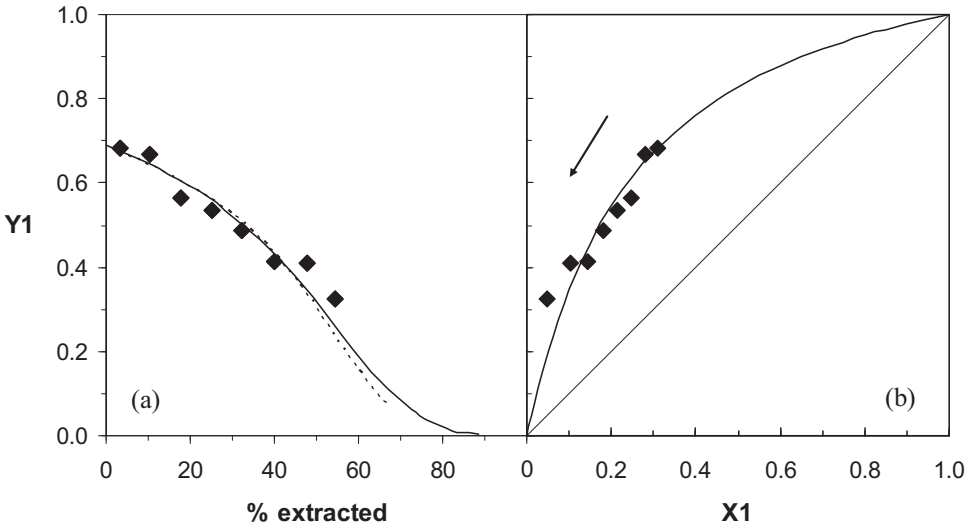

Fig. 7. Semicontinuous fractionation of peppermint oil at 313 K and 85 bar. (a) Extract-phase composition (CO_2-free basis) vs. extraction degree. (b) Equilibrium diagram (Y_1 vs. X_1). (♦) Experimental data, (—) simulation with Rayleigh equation using constant relative volatility, (—) GC-EOS predictions. (The arrow indicates the fractionation process direction.)

the calculation of both diagrams. Even this first analysis could be avoided if a reliable model for predicting the relative volatility is available.

Ternary phase equilibrium information, including supercritical CO_2, is presented in Fig. 8. GC-EOS predictions are shown and compared to the experimental results for the gas phase obtained from the semicontinuous fractionation experiment. As it can be seen, the model correctly describes the gas phase behavior, and predicts a significant dissolution of CO_2 in the liquid phase, between 40 and 50% wt. at these conditions.

4.3. Continuous countercurrent fractionation

Fig. 9 shows the schematic diagram of the studied fractionation configuration. It consists of a multistage column with the solvent feed (S) at the bottom and the oil feed (F) at the top or at an intermediate stage. The raffinate (R) and extract (E) streams are recovered at the bottom and top, respectively. The extract is condensed in a separation vessel operating at 280 K and 35 bar and can be partially recycled to the top of the column as an external reflux. Separator conditions were chosen in order to obtain a quantitative condensation of oil components and a sufficiently pure CO_2 stream. The solvent recovery system was not analyzed.

Fractionation performance was evaluated taking into account different criteria. The search for optimal or recommended conditions aims at maximizing raffinate purity and recovery (in terms of piperitenone or fraction 2) while minimizing solvent consumption and investment costs. Solvent consumption was evaluated by means of the solvent-to-feed ratio (*S*/*F*), in order to generalize the analysis independently of the required column throughput.

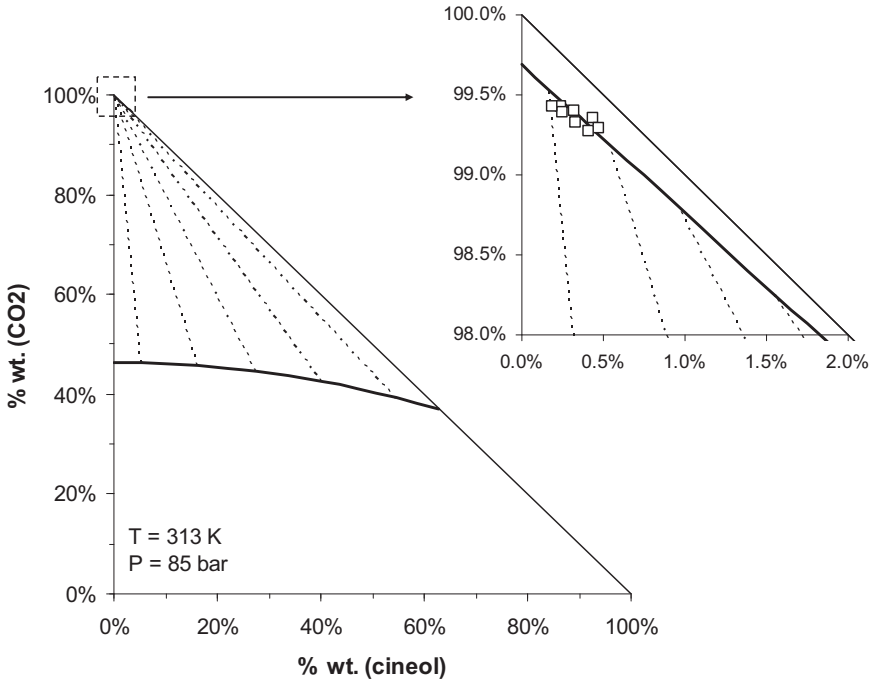

Fig. 8. Ternary diagram for the system CO_2 + 1,8-cineol + piperitenone at 313 K and 85 bar. (□) Experimental data for gas phase, (—) GC-EOS predictions, (- - -) tie lines.

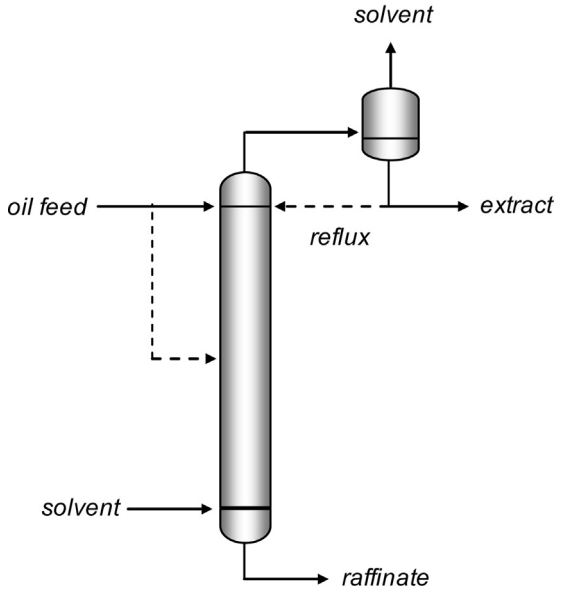

Fig. 9. Countercurrent fractionation scheme. Solid lines: simple countercurrent mode. Dotted lines: countercurrent mode with external reflux.

Investment costs are mainly related to the number of theoretical stages (N) and the column diameter, the latter depending basically on solvent flow rate and density.

In a first analysis, a simple countercurrent operation in an isothermal 10-stage column was investigated. Preliminary simulations showed that further increasing the number of stages did not improve the column performance in terms of product quality. Fig. 10(a) and (b) shows the predicted conditions (*S*/*F* ratio and operation pressure) for two specified values of piperitenone purity in the raffinate product (99 and 95% wt.) operating at 313 and 323 K, respectively. These temperatures were selected based on the preliminary experimental results and model predictions. It can be seen that a higher *S*/*F* ratio is needed when operating at lower pressures. Fig. 10 also shows that the piperitenone loss in the extract (in % wt.) increases with pressure due to the increase in CO_2 solvent power. Due to this opposite behavior of *S*/*F* ratio and piperitenone loss, the best choice of pressure will depend on further considerations. For example, for a product purity of 99% wt., if a maximum limit of 15% of piperitenone loss is fixed, the required operation conditions will be 90 bar and *S*/*F* = 98 kg/kg at 313 K, and 93 bar and *S*/*F* = 93 kg/kg at 323 K. At 313 K and 90 bar, CO_2 density is 485 kg/m^3, while at 323 K and 93 bar it is 317 kg/m^3. Therefore, although a higher *S*/*F* ratio is needed, the volumetric flow rate will be lower at 313 K (0.20 vs. 0.29 m^3 per kg oil feed), reducing the required column diameter and the associated investment costs. It can also be seen that it is not possible to reduce the piperitenone loss in the extract below 10% with this purity requirement within the operative region. If purity requirement is relaxed to 95% wt., a lower *S*/*F* ratio is needed for a given pressure, and the piperitenone loss in the extract decreases.

To avoid partial or total selectivity loss, it is fundamental to keep heterogeneous (biphasic) conditions across the entire column. CO_2 solvent power increases with pressure; hence, there will be a maximum operative value to avoid complete miscibility. In general, the maximum pressure will shift to higher values with temperature, due to its effect on solvent density, as it can be seen in Fig. 9 for the 10-stage column operating at 313 and 323 K. It can also be noticed that this maximum pressure decreases with *S*/*F* ratio for a given temperature, due to the effect of CO_2 composition on the ternary phase equilibrium. The operation should be performed below the maximum pressure, in order to avoid entering the homogeneous region and to keep a density difference between gas and

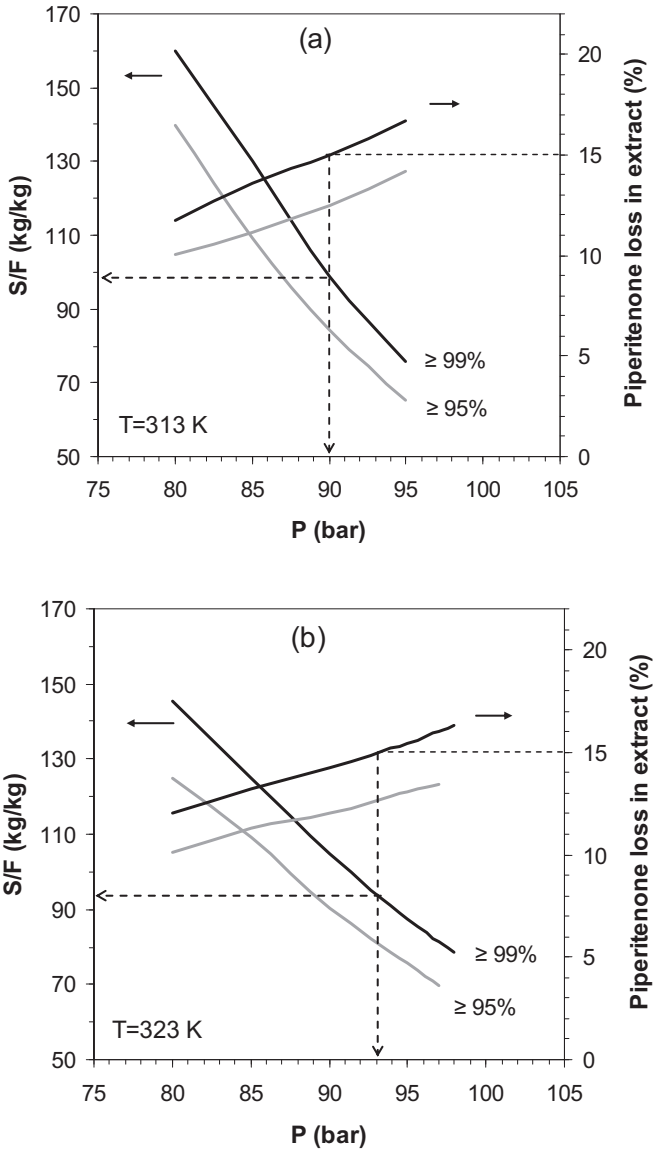

Fig. 10. Solvent-to-feed ratio (*S*/*F*) and piperitenone loss in the extract as a function of operation pressure for 99 and 95% wt. of piperitenone purity in raffinate product. Predictions for a 10-stage simple countercurrent column operating at (a) 313 K and (b) 323 K.

liquid phase high enough to ensure a countercurrent flow without entrainment or flooding risks. As it can be seen in Fig. 11, the previously selected operation conditions are well below this limit.

In order to increase piperitenone recovery, the use of an external reflux was studied. It has been demonstrated that the possibility of simultaneously achieving a high recovery in the extract and raffinate phase in simple countercurrent columns is limited by the relative volatility between the components or fractions to be separated at the prevailing column conditions [19]. A limited reflux of the condensed extract product can improve the recovery of the less volatile component in the raffinate by around 10%, as reported for the fractionation of *T. minuta* and *S. officinalis* essential oils [27].

The operation of a 15-stage countercurrent column with oil feed at stage 5 and external reflux at the top was simulated. Temperature, pressure and *S*/*F* ratio were kept constant at the previously selected values for the simple countercurrent mode (313 K, 90 bar, 98 kg/kg). Table 8 shows the predicted results using a reflux ratio of 0.5, in comparison with the simple countercurrent mode. It can be seen that by using this reflux ratio piperitenone recovery is

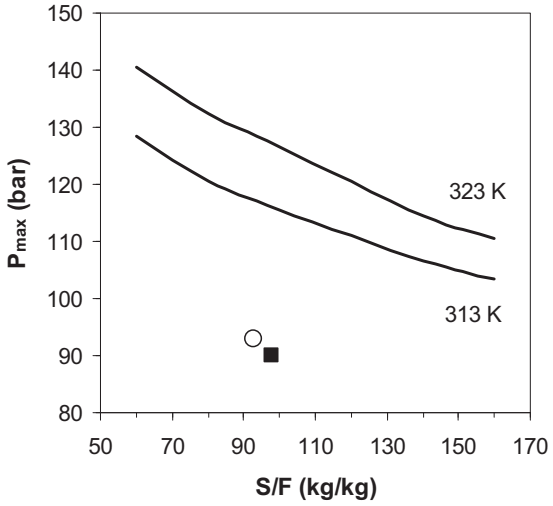

Fig. 11. Solid lines: maximum operation pressure as a function of solvent-to-feed ratio (*S*/*F*) and temperature, for ensuring biphasic conditions along the column. Dots: recommended operation conditions (■) at 313 K and (○) at 323 K. Predictions for a 10-stage simple countercurrent column.

Table 8
Continuous countercurrent fractionation of peppermint oil. Selected operation conditions and prediction of piperitenone purity and recovery in raffinate product.

	Simple CC	CC with external reflux
Column temperature (K)	313	313
Column pressure (bar)	90	90
S/*F* ratio (kg/kg)	98	98
Number of stages	10	15
Feed stage	1	5
Separator temperature (K)	–	280
Separator pressure (bar)	–	35
Reflux ratio	–	0.5
Piperitenone in raffinate, CO_2-free (% wt.)	99.1	98.6
Piperitenone recovery (%)	85.0	91.1

increased from 85% to 91.1%, for a raffinate product of similar quality.

Finally, it is important to consider also the influence of feed oil composition. In general, qualitative and quantitative changes in the natural composition of herbal essential oils are expectable due to geographical, environmental and genetic factors, as well as extraction methods and conditions. These variations between lots usually require the adjustment of fractionation conditions, as the selectivity and phase scenario can be drastically modified. In this case, the effect of quantitative variations in the piperitenone content in the feed oil is analyzed. It can be seen in Fig. 12 that the predicted pressure limit for biphasic conditions shifts to higher values as the piperitenone content increases, at constant temperature and *S*/*F* ratio. This is consistent with the fact that piperitenone is the less soluble component in supercritical CO_2, due to its lower volatility, expanding, therefore, the heterogeneous region. In the same way, the predicted relative volatility of 1,8-cineol with respect to piperitenone increases with piperitenone content. The separation performance and the operative region are limited by these effects, making the purification of piperitenone from cineol-rich feeds more difficult. In these cases, larger columns and greater solvent flow rates might be required, as well as higher

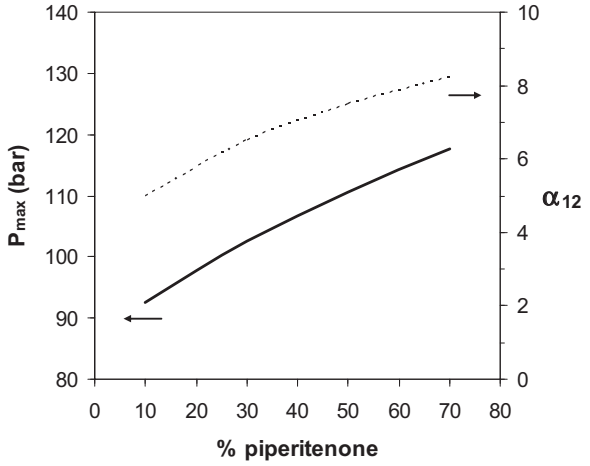

Fig. 12. Influence of feed oil composition on a 10-stage column operating at simple countercurrent mode at *T* = 313 K and *S*/*F* = 98 kg/kg. (—) Maximum pressure for biphasic conditions. (- - -) Mean column relative volatility at 90 bar.

temperatures, in order to operate at biphasic conditions and increased selectivity.

5. Conclusions

In this work, a study concerning the fractionation of a piperitenone-rich peppermint essential oil with supercritical CO_2 was presented. The influence of operation temperature and solvent density on fractionation selectivity and gas loading was studied experimentally in a dynamic high-pressure apparatus with a minimum number of runs. Based on the previous results, a semicontinuous fractionation of a sample of oil was performed at 313 K and 85 bar, analyzing the gas phase composition until the total removal of volatile compounds (mainly 1,8-cineol). The phase equilibrium behavior of the system was described with the GC-EOS model, getting a good agreement between experimental results and model predictions. For simplicity, the oil was represented as a pseudo-binary mixture of 1,8-cineol and piperitenone, based on their volatility behavior. The semicontinuous fractionation was modeled using the well-known Rayleigh equation for a pseudo-binary system, as a fast method for predicting the process evolution with minimal experimental information.

Continuous countercurrent fractionation was also studied by computer-aided simulation of a multistage column, using the GC-EOS thermodynamic model and applying phase equilibrium engineering concepts. In a first analysis, a 10-stage column operating under simple countercurrent mode was studied. An opposite behavior with respect to the operation pressure was predicted for the solvent/feed ratio and the piperitenone loss in the extract; therefore, optimal conditions had to be searched for. For a 99% wt. piperitenone purity in the raffinate and a maximum admissible loss of 15% in the extract, the best operating conditions were 313 K, 90 bar and a solvent-to-feed ratio of 98 kg/kg, based on minimization of solvent consumption and column diameter. The effect of an external reflux was also analyzed. Piperitenone recovery increased to approx. 91% by using a reflux ratio of 0.5 in a 15-stage column at the previously selected conditions. Finally, the effect of quantitative variations in oil composition was evaluated. The results indicate a reduction in the operative pressure range and separation selectivity as piperitenone content decreases.

In conclusion, supercritical CO_2 fractionation is proposed as an interesting alternative for the recovery of piperitenone and other biologically active ketones from low-menthol or dementholized mint oils. Semicontinuous fractionation can be useful

for preparative purposes (for example, sample purification for biological activity assays) or for small-scale processing of variable feeds. On the other hand, solvent-free ketone-rich fractions with potential value as biopesticides can be obtained at industrial scale in a simple countercurrent column optimized according to phase equilibrium considerations.

Acknowledgements

This work was carried out with the financial support of CONICET (Argentina). The authors gratefully thank Prof. Dr. Julio Zygadlo for providing the sample of *M. piperita* essential oil.

References

[1] R.M. Sheldon, The global mint industry. Market dynamics, consumer trends, mint oil supply and opportunities for new innovation, in: Proceedings of the IFEAT International Conference, Montreal, Canada, 2008.
[2] J.C. Yori, D.L. Manuale, A.J. Marchi, J.M. Grau, Liquid-phase hydrogenation of dementholized peppermint oil on Pt/Al_2O_3 catalysts. Part I: A study of catalyst performance, Applied Catalysis A: General 275 (2004) 221–226.
[3] N. Ravasio, F. Zaccheria, A. Fusi, R. Psaro, One pot selective hydrogenation and dynamic kinetic resolution over Cu/Al_2O_3: a way to (−)-menthol starting from low value mint oils, Applied Catalysis A: General 315 (2006) 114–119.
[4] P. Kumar, S. Mishra, A. Malik, S. Satya, Insecticidal properties of *Mentha* species: a review, Industrial Crop and Products 34 (2011) 802–817.
[5] A. Sivropoulou, S. Kokkini, T. Lanaras, M. Arsenakis, Antimicrobial activity of mint essential oils, J. Agricultural and Food Chemistry 43 (1995) 2384–2388.
[6] G. Franzios, M. Mirotsou, E. Hatziapostolou, J. Kral, Z.G. Scouras, P. Mavragani-Tsipidou, Insecticidal and genotoxic activities of mint essential oils, J. Agricultural and Food Chemistry 45 (1997) 2690–2694.
[7] G. Iscan, N. Kirimer, M. Kurkcuoglu, K.H. Can Baser, F. Demirci, Antimicrobial screening of *Mentha piperita* essential oils, J. Agricultural and Food Chemistry 50 (2002) 3943–3946.
[8] C. Regnault-Roger, C. Vincent, J.T. Arnason, Essential oils in insect control: low-risk products in a high-stakes world, Annual Review of Entomology 57 (2012) 405–424.
[9] L.S. Nerio, J. Olivero-Verbel, E. Stashenko, Repellent activity of essential oils: a review, Bioresource Technology 101 (2010) 372–378.
[10] D.P. Papachristos, D.C. Stamopoulos, Repellent, toxic and reproduction inhibitory effects of essential oil vapours on *Acanthoscelides obtectus* (Say) (Coleoptera: Bruchidae), J. Stored Products Research 38 (2002) 117–128.
[11] A.K. Tripathi, V. Prajapati, S. Kumar, Bioactivities of L-carvone, D-carvone and dihydrocarvone toward three stored product beetles, J. Economic Entomology 96 (2003) 1594–1601.
[12] S. Lee, C. Peterson, J. Coats, Fumigation toxicity of monoterpenoids to several stored product insects, J. Stored Products Research 39 (2003) 77–85.
[13] J.M. Herrera, M.P. Zunino, Y. Massuh, R.P. Pizzollito, J.S. Dambolena, N.A. Gañán, J.A. Zygadlo, Fumigant toxicity of five essential oils rich in ketones against *Sitophilus zeamais* (Motschulsky), Agriscientia 31 (2014) 35–41.
[14] G. Brunner, Counter-current separations (review), J. Supercritical Fluids 47 (2009) 574–582.
[15] M. Sato, M. Kondo, M. Goto, A. Kodama, T. Hirose, Fractionation of citrus oil by supercritical countercurrent extractor with side-stream withdrawal, J. Supercritical Fluids 13 (1998) 317–331.
[16] E. Reverchon, A. Marciano, M. Poletto, Fractionation of a peel oil key mixture by supercritical CO_2 in a continuous tower, Industrial & Engineering Chemistry Research 36 (1997) 4940–4948.
[17] M. Budich, S. Heilig, T. Wesse, V. Leibküchler, G. Brunner, Countercurrent deterpenation of citrus oils with supercritical CO_2, J. Supercritical Fluids 14 (1999) 104–114.
[18] F. Gironi, M. Maschietti, Supercritical carbon dioxide fractionation of lemon oil by means of a batch process with an external reflux, J. Supercritical Fluids 35 (2005) 227–234.
[19] S. Diaz, S. Espinosa, E.A. Brignole, Citrus peel oil deterpenation with supercritical fluids: optimal process and solvent cycle design, J. Supercritical Fluids 35 (2005) 49–61.
[20] E. Reverchon, A. Ambruosi, F. Senatore, Isolation of peppermint oil using supercritical CO_2 extraction, Flavour and Fragrance J. 9 (1994) 19–23.
[21] B.C. Roy, M. Goto, A. Kodama, T. Hirose, Supercritical CO_2 extraction of essential oils and cuticular waxes from peppermint leaves, J. Chemical Technology and Biotechnology 67 (1996) 21–26.
[22] K. Ansari, I. Goodarznia, Optimization of supercritical carbon dioxide extraction of essential oil from spearmint (*Mentha spicata* L.) leaves by using Taguchi methodology, J. Supercritical Fluids 67 (2012) 123–130.
[23] O. Köse, U. Akman, Ö. Hortacsu, Semi-batch deterpenation of origanum oil by dense carbon dioxide, J. Supercritical Fluids 18 (2000) 49–63.
[24] S. Varona, A. Martin, M.J. Cocero, T. Gamse, Supercritical carbon dioxide fractionation of Lavandin essential oil: experiments and modeling, J. Supercritical Fluids 45 (2008) 181–188.
[25] P.C. Simoes, H.A. Matos, P.J. Carmelo, E. Gomes de Acevedo, M. Nunes da Ponte, Mass transfer in countercurrent packed columns: application to supercritical CO_2 extraction of terpenes, Industrial & Engineering Chemistry Research 34 (1995) 613–618.
[26] N. Gañán, E.A. Brignole, Fractionation of essential oils with biocidal activity using supercritical CO_2 – experiments and modeling, J. Supercritical Fluids 58 (2011) 58–67.
[27] N. Gañán, E.A. Brignole, Supercritical carbon dioxide fractionation of *T. minuta* and *S. officinalis* essential oils: experiments and process analysis, J. Supercritical Fluids 78 (2013) 12–20.
[28] H. Sovová, J. Jez, Solubility of menthol in supercritical carbon dioxide, J. Chemical and Engineering Data 39 (1994) 840–841.
[29] H. Sovová, R.P. Stateva, A.A. Galushko, High-pressure equilibrium of menthol + CO_2, J. Supercritical Fluids 41 (2007) 1–9.
[30] K.H. Kim, J. Hong, Equilibrium solubilities of spearmint oil components in supercritical carbon dioxide, Fluid Phase Equilibria 164 (1999) 107–115.
[31] J. da Cruz Francisco, B. Sivik, Solubility of three monoterpenes, their mixtures and eucalyptus leaf oils in dense carbon dioxide, J. Supercritical Fluids 23 (2002) 11–19.
[32] H.A. Matos, E. Gomes de Acevedo, Phase equilibria of natural flavours and supercritical solvents, Fluid Phase Equilibria 52 (1989) 357–364.
[33] A.K. Tripathi, V. Prajapati, A. Ahmad, K.K. Aggarwal, S.P.S. Khanuja, Piperitenone oxide as toxic, repellent, and reproduction retardant toward malarial vector *Anopheles stephensi* (Diptera: Anophelinae), J. Medical Entomology 41 (2004) 691–698.
[34] E.A. Brignole, S. Pereda, Phase Equilibrium Engineering, Elsevier, Amsterdam, The Netherlands, 2013.
[35] S. Skjold-Jorgensen, Group contribution equation of state (GC-EOS): a predictive method for phase equilibrium computations over wide ranges of temperatures and pressures up to 30 MPa, Industrial & Engineering Chemistry Research 27 (1988) 110–118.
[36] P.R. Adams, Identification of Essential Oil Components by Gas Chromatography/Mass Spectrometry, 4th ed., Allured Publishing, Carol Stream, IL/USA, 2007.
[37] F. Temelli, J. O'Connell, C. Chen, R. Braddock, Thermodynamic analysis of supercritical carbon dioxide extraction of terpenes from cold-pressed orange oil, Industrial & Engineering Chemistry Research 29 (1990) 618–624.
[38] S. Espinosa, Ph.D. thesis, Universidad Nacional del Sur, Bahía Blanca, Argentina, 2001.
[39] B.E. Poling, J.M. Prausnitz, J.P. O'Connell, The Properties of Gases and Liquids, 5th ed., McGraw-Hill, New York/USA, 2001.
[40] T. Fornari, Revision and summary of the group contribution equation of state parameter table: application to edible oil constituents, Fluid Phase Equilibria 262 (2007) 187–209.
[41] J.D. Seader, E.J. Henley, Separation Process Principles, 2nd ed., John Wiley and Sons Inc., Somerset, New Jersey/USA, 1998.
[42] M.L. Michelsen, The isothermal flash problem. Part II: Phase-split calculation, Fluid Phase Equilibria 9 (1982) 21–40.
[43] E.A. Brignole, P.M. Andersen, A. Fredenslund, Supercritical fluid extraction of alcohols from water, Industrial & Engineering Chemistry Research 26 (1987) 254–261.
[44] S. Espinosa, S.B. Bottini, E.A. Brignole, Process analysis and phase equilibria for the removal of chemicals from fatty oils using near-critical solvents, Industrial & Engineering Chemistry Research 39 (2000) 3024–3033.
[45] S. Espinosa, S. Díaz, E.A. Brignole, Thermodynamic modeling and process optimization of supercritical fluid fractionation of fish oil fatty acid ethyl esters, Industrial Engineering & Chemistry Research 41 (2002) 1516–1527.
[46] http://webbook.nist.gov/chemistry/fluid/